Original article

Epimedin B exhibits pigmentation by increasing tyrosinase family proteins expression, activity, and stability

Chen Hong [a], Yifan Zhang [a], Lili Yang [b], Haoyang Xu [c], Kang Cheng [d], Zhi Lv [d], Kaixian Chen [a], Yiming Li [a, **], Huali Wu [a, *]

[a] Department of TCM Chemistry, School of Pharmacy, Shanghai University of Traditional Chinese Medicine, Shanghai, 200000, China
[b] Department of Dermatology, Shuguang Hospital Affiliated to Shanghai University of Traditional Chinese Medicine, Shanghai, 200000, China
[c] International Education College, Shanghai University of Traditional Chinese Medicine, Shanghai, 200000, China
[d] Shanghai Inoherb Cosmetics Co., Ltd., Shanghai, 200000, China

ARTICLE INFO

ABSTRACT

Epimedin B (EB) is one of the main flavonoid ingredients present in *Epimedium brevicornum* Maxim., a traditional herb widely used in China. Our previous study showed that EB was a stronger inducer of melanogenesis and an activator of tyrosinase (TYR). However, the role of EB in melanogenesis and the mechanism underlying the regulation remain unclear. Herein, as an extension to our previous investigation, we provide comprehensive evidence of EB-induced pigmentation *in vivo* and *in vitro* and elucidate the melanogenesis mechanism by assessing its effects on the TYR family of proteins (TYRs) in terms of expression, activity, and stability. The results showed that EB increased TYRs expression through microphthalmia-associated transcription factor-mediated p-Akt (referred to as protein kinase B (PKB))/glycogen synthase kinase 3β (GSK3β)/β-catenin, p-p70 S6 kinase cascades, and protein 38 (p38)/mitogen-activated protein (MAP) kinase (MAPK) and extracellular regulated protein kinases (ERK)/MAPK pathways, after which EB increased the number of melanosomes and promoted their maturation for melanogenesis in melanoma cells and human primary melanocytes/skin tissues. Furthermore, EB exerted repigmentation by stimulating TYR activity in hydroquinone- and *N*-phenylthiourea-induced TYR inhibitive models, including melanoma cells, zebrafish, and mice. Finally, EB ameliorated monobenzone-induced depigmentation *in vitro* and *in vivo* through the enhancement of TYRs stability by inhibiting TYR misfolding, TYR-related protein 1 formation, and retention in the endoplasmic reticulum and then by downregulating the ubiquitination and proteolysis processes. These data conclude that EB can target TYRs and alter their expression, activity, and stability, thus stimulating their pigmentation function, which might provide a novel rational strategy for hypopigmentation treatment in the pharmaceutical and cosmetic industries.

1. Introduction

Mammalian skin and hair pigmentation occurs as a result of various cellular biochemical processes and the synergistic action of two cell types: melanocytes (responsible for melanin biosynthesis) and keratinocytes (responsible for the proper distribution of the melanin pigment transferred from the melanocytes). Owing to its strong light-absorbing property, melanin present in the skin and hair provides photoreceptor shielding, thermoregulation, photoprotection, camouflage, and coloring effect [1].

Melanin is a pigment synthesized within membrane-bound intracellular compartments, called melanosomes, which are specialized cytoplasmic lysosomal-related organelles of melanocytes. Melanosomes are typically divided into four stages according to their structure, number, quality, and arrangement. Nonpigmented stage I vacuoles, which are derived from the endosomal system, acquire internal striations to form stage II melanosomes. Melanin synthesis begins in stage III melanosomes, after which the melanosomes eventually mature into the fully melanized stage IV lobules containing accumulated melanin [2]. Melanized melanosomes that are fully filled with melanin are carried by dendrites and transferred from melanocytes to keratinocytes, wherein the melanin pigment is retained to provide color to the skin and hair [3].

Melanogenesis is a complex and multistep process catalyzed by three major pigmentation enzymes: tyrosinase (TYR), TYR-related protein 1 (TYRP1), and dopachrome tautomerase (DCT). TYR, TYRP1, and DCT belong to the TYR family of proteins (TYRs). Mature TYRs enter intracellular trafficking and are carried to the melanosomes, wherein the melanin pigment is synthesized. While all three enzymes (TYR, TYRP1, and DCT) are involved in melanogenesis, only TYR is exclusively necessary for melanogenesis. The hydroxylation of L-tyrosine to L-dopa, catalyzed by TYR, is the rate-limiting step in melanin synthesis [4]. Microphthalmia-associated transcription factor (MITF) is a unique member of the microphthalmia family and the master regulator of melanogenesis-related gene expression [5]. Generally, upregulation on TYRs expression directly by MITF or activation on TYR activity is regarded as effective means for melanin production.

In addition to the synthesis of TYRs, the degradation of TYRs is equally tightly coupled to melanogenesis. This process affects almost all proteins, including TYRs, which have a direct and dramatic effect on pigmentation. Studies on carbohydrate modifications of TYRs have showed that TYRs degraded in endoplasmic reticulum (ER) are proteolyzed by proteasomes through the ER-associated protein degradation (ERAD) pathway [6]. In albino melanocytes or amelanotic melanoma cells, the aberrant retention of TYRs in the ER and their degradation are achieved by the quality-control machinery [7]. Thus, modulation of the stability of TYRs has clinical significance for pigmentation.

In our previous study, we reported that epimedin B (EB; PubChem CID: 5748393), an abundant, low-toxicity flavonoid ingredient presenting in *Epimedium brevicornum* Maxim., is a strong inducer of melanogenesis and activator of TYRs [8]. However, no studies have evaluated the role of EB in melanin pigment synthesis and the mechanism underlying the regulation. In this study, as an extension to our previous investigation, we provide comprehensive evidence of EB-induced pigmentation *in vivo* and *in vitro* and elucidate the melanogenesis mechanism through the effects on TYRs in terms of three aspects (expression, activity, and stability). Our findings demonstrated that EB can target TYRs and stimulate them to exert pigmentation function, which might provide a novel rational strategy for hypopigmentation treatment in the pharmaceutical and cosmetic industries.

2. Materials and methods

2.1. Chemicals and reagents

EB (Standard Technology Co., Ltd., Shanghai, China), isobutylmethylxanthine (IBMX) (Sigma-Aldrich, Shanghai, China), α-melanocyte-stimulating hormone (α-MSH) (Sigma-Aldrich), L-dopa (Sigma-Aldrich), Dulbecco's modified Eagle medium (DMEM) (Thermo Fisher Scientific Inc., Waltham, MA, USA), Medium 254 (Thermo Fisher Scientific Inc.), Williams' Medium E (Thermo Fisher Scientific Inc.), penicillin-streptomycin solution (Beyotime Biotechnology, Shanghai, China), Triton X-100 (Scigrace Biotech Co., Ltd., Shanghai, China), bovine serum albumin (BSA) (Scigrace Biotech Co., Ltd.), mushroom TYR (Thermo Fisher Scientific Inc.), hydroquinone (HQ) (Aladdin Biochemical Technology Co., Ltd., Shanghai, China), monobenzone (Aladdin Biochemical Technology Co., Ltd.), animal emulsion cream (Bloomage Biotechnology Co., Ltd., Shanghai, China), and cycloheximide (CHX) (GlpBio Technology, Montclair, CA, USA) were used. Other reagents were purchased from China National Pharmaceutical Group Corporation (Shanghai, China).

2.2. Cell and tissue culture

B16F10 and MNT-1 cells were cultured in DMEM containing 10% and 15% fetal bovine serum and 1% penicillin/streptomycin at 37 °C and 5% CO_2. Primary human melanocytes were cultured in an M254 medium containing a human melanocyte growth supplement. Normal human/depigmented donor skin tissues were cultured in Williams' Medium E without fetal bovine serum. Experiments on human material were approved by the local ethics committee and donor, and were complied with the privacy rights of human subjects (Approval No.: 2019–735–90–01 in IRB of Shuguang Hospital affiliated with Shanghai University of Traditional Chinese Medicine, Shanghai, China). Normal human foreskin-derived epidermal melanocytes were obtained from young male adult foreskins (ethnicity: Han/aged: 18–22 years). The detailed protocol has been published in a previous study [9].

2.3. Melanin content quantification

Melanin content was measured according to a previously described method [10]. Cells were treated with IBMX (100 μM), α-MSH (100 nM), EB (25, 50, and 100 μM), HQ (25 μM), and monobenzone (5 μM) for 72 h (in monobenzone-induced depigmentation, the B16F10 cells were prestimulated with IBMX/α-MSH), and with EB (100 μM) for 12, 24, 48, and 72 h. The total melanin content in cell pellet was dissolved in 100 μL of 1 N NaOH/10% dimethyl sulfoxide. After incubation for 2 h at 80 °C, the absorbance of the solubilized melanin was measured at 405 nm using a microplate reader (BioTek Instruments, Montpellier, VT, USA).

2.4. Skin tissue staining

Cultured normal human/depigmented donor skin tissues were treated with EB (1 mM for a week) at 37 °C and 5% CO_2. The skin tissues were washed thrice with phosphate-buffered saline (PBS), after which they were fixed in 4% (V/V) paraformaldehyde, dehydrated, and embedded in paraffin. The paraffin-embedded tissues were then sectioned into 5-μm-thick slices using a microtome and stained using the Masson-Fontana dye kit (Sbjbio Biotechnology Co., Ltd., Nanjing, China) and anti-HMB45 (referred to as melanoma gp100) (Santa Cruz Biotechnology, Inc., Dallas, TX, USA) according to the manufacturer's instructions. Images were captured using a microscope (BX43F; Olympus Corporation, Tokyo, Japan).

Mouse dorsal skin tissues were obtained, after which they were fixed in 4% (V/V) paraformaldehyde, dehydrated, and embedded in paraffin. The paraffin-embedded skin tissues were then sectioned into 5-μm-thick slices using a microtome and stained using the hematoxylin-eosin (H&E) dye and anti-TYR (Abcam Trading Co., Ltd., Shanghai, China), followed by incubation with the corresponding fluorescent dye-conjugated secondary antibodies (Servicebio Technology Co., Ltd., Wuhan, China), according to the manufacturer's instructions. Images were captured using a microscope (BX43F; Olympus Corporation).

2.5. Immunofluorescence staining and transmission electron microscopy

Cells were cultured on coverslips in a 12-well plate and treated with EB (100 μM) for 72 h. The supernatant was then discarded, and cells were washed thrice with PBS, after which they were fixed in 4% (V/V) paraformaldehyde for 10 min and treated with 0.1% (V/V) Triton for 5 min; they were sealed with 5% (V/V) BSA at room

temperature for 1 h. The cells were incubated with anti-HMB45 (Santa Cruz Biotechnology, Inc.), anti-TYR (Abcam Trading Co., Ltd.), fluorescein isothiocyanate (FITC)-phalloidin (Enzo Life Sciences, Inc., New York City, NY, USA), anti-TYRP1 (Abcam Trading Co., Ltd.), anti-calnexin (Santa Cruz Biotechnology, Inc.), and anti-26S proteasome α (Santa Cruz Biotechnology, Inc.) at 4 °C overnight, followed by incubation with fluorescent dye-conjugated secondary antibodies FITC-AffiniPure Goat (Yeasen Biotechnology Co., Ltd., Shanghai, China) and Rhodamine AffiniPure (Yeasen Biotechnology Co., Ltd.) for 1 h at room temperature. The cells were washed thrice with PBS and then mounted with a mounting medium (with 4′,6-diamidino-2-phenylindole (DAPI); Thermo Fisher Scientific Inc.). Images were captured using a confocal microscope (SP8; Leica, Weztlar, Germany).

Cultured normal human skin tissues were treated with EB (1 mM) and monobenzone (60 μM) for a week at 37 °C and 5% CO_2. The skin tissues were washed thrice with PBS, after which they were fixed in 4% (*V/V*) paraformaldehyde, dehydrated, and embedded in paraffin. The paraffin-embedded tissues were sectioned into 5-μm-thick slices using a microtome and stained with anti-HMB45 (Santa Cruz Biotechnology, Inc.) and anti-TYR (Abcam Trading Co., Ltd.), followed by incubation with the corresponding fluorescent dye-conjugated secondary antibodies (Servicebio Technology Co., Ltd.), according to the manufacturer's instructions (Servicebio Technology Co., Ltd.). Images were captured using a confocal microscope (SP8; Leica).

Cells were treated with EB (100 μM) for 72 h and were then centrifuged; the pellet was collected and fixed in 2.5% (*V/V*) glutaraldehyde. The fixed cells were washed thrice with buffer for 10−20 min, after which they were fixed again in 1% osmic acid, dehydrated with gradient ethanol, embedded in paraffin, and stained. Images were captured using a transmission electron microscope (Tecnai G2 Spirit BioTWIN; FEI, Hillsboro, OR, USA).

2.6. RNA transcriptome sequencing

Normal human foreskin-derived epidermal melanocytes were obtained from young male adult foreskin tissues (ethnicity: Han/aged 18−22 years). The detailed protocol has been published in our previous study [9]. Primary human melanocytes were treated with EB (100 μM) for 72 h. Total RNA was isolated from the cells for the construction of RNA-sequencing libraries. The quality of the constructed RNA libraries was evaluated using Agilent 2200 TapeStation (Agilent Technologies Inc., Palo Alto, CA, USA). Library sequencing was performed on the HiSeq 4000 sequencing platform (Novogene Co., Ltd., Beijing, China). Clustering was performed in a cBot cluster generation system using the TruSeq PE Cluster Kit v3-cBot-HS (Illumina, Inc., San Diego, CA, USA).

2.7. Western blotting and cAMP content quantification

Cells were lysed with cell lysis buffer (containing 1% (*V/V*) phenylmethylsulfonyl fluoride (PMSF)), and total protein was extracted. The total protein content was determined using the bicinchoninic acid assay (BCA) Protein Assay kit (Beyotime Biotechnology). The extracted protein was separated by sodium dodecyl sulfate-polyacrylamide gel electrophoresis (SDS-PAGE), then transferred to polyvinylidene difluoride membrane and sealed with 5% (*V/V*) BSA for 1−2 h at room temperature. The membrane was incubated with anti-p-MITF (ImmunoWay Biotechnology Company, Plano, TX, USA), anti-MITF (Abcam Trading Co., Ltd.), anti-TYR (Abcam Trading Co., Ltd.), anti-TYRP1 (Abcam Trading Co., Ltd.), anti-DCT (Abcam Trading Co., Ltd.), anti-melanoma antigen (Melan-A) (Abcam Trading Co., Ltd.), anti-Actin (Sigma-Aldrich), anti-protein kinase A (PKA) (Cell Signaling Technology, Inc., Boston, MA, USA), anti-phosphoinositide

3-kinase (PI3K) (Cell Signaling Technology, Inc.), anti-p-AKT (referred to as protein kinase B (PKB)) (Cell Signaling Technology, Inc.), anti-AKT (Cell Signaling Technology, Inc.), anti-glycogen synthase kinase 3β (GSK3β; Cell Signaling Technology, Inc.), anti-β-catenin (ImmunoWay Biotechnology Company), anti-p-p70 S6 (Cell Signaling Technology, Inc.), anti-p70 S6 (Cell Signaling Technology, Inc.), anti-p-c-Jun N-terminal kinase (JNK)/JNK (Cell Signaling Technology, Inc.), anti-p-protein 38 (p38)/p38 (Cell Signaling Technology, Inc.), anti-p-extracellular regulated protein kinases (ERK)/ERK (Cell Signaling Technology, Inc.), anti-Ras-related protein Rab-27A (Rab27a) (Cell Signaling Technology, Inc.), anti-Ras homolog family member A (RhoA) (Abcam Trading Co., Ltd.), and anti-cell division cycle 42 (CDC42) (Abcam Trading Co., Ltd.) at 4 °C overnight, and then, the membrane was probed with the corresponding secondary antibody at room temperature for 1 h. The signals were visualized using Tanon 4600SF (Tanon Technology Co., Ltd., Shanghai, China) and determined by quantitative analysis of digital images of gels using ImageJ (version 1.8.0).

Cells were treated with EB (100 μM) for 0, 0.5, 1, 3, and 6 h, after which they were lysed with cell lysis buffer (containing 1% (*V/V*) PMSF); total protein was extracted, and its content was determined using the BCA Protein Assay kit (Beyotime Biotechnology). The cell lysate was incubated with the contents of the cyclic AMP (cAMP) enzyme-linked immunosorbent assay kit (Thermo Fisher Scientific Inc.), according to the cAMP kit manufacturer's instructions; the absorbance was measured at 450 nm using a multimode reader (BioTek Instruments).

2.8. Quantitative reverse transcription-polymerase chain reaction (PCR)

Total RNA was extracted using RNA isolater extraction reagent (Vazyme Biotech Co., Ltd., Nanjing, China) and determined according to the manufacturer's protocol. Reverse transcription of RNA into complementary DNA using the SuperScript™ First-Strand Synthesis System (Thermo Fisher Scientific Inc.). Real time-PCR (RT-PCR) was performed using a PCR system (7500 Fast; Thermo Fisher Scientific Inc.) with SYBR Green PCR Master Mix (Vazyme Biotech Co., Ltd.). Primer sequences were provided in the Supplementary data.

2.9. Mushroom tyrosinase and cellular tyrosinase activity assay

Different concentrations of EB were prepared with PBS (pH 6.8). A mixture solution (200 μL in each well) comprising mushroom TYR (100 U; 100 μL; EC 1.14.18.1), L-dopa (50 μL; 0.5 mg/mL), and EB (50 μL; 1, 10, 25, 50, and 100 μM) was prepared. The mixture solution was incubated at 25 °C in the dark, and the absorbance was measured at 475 nm per change in time (1 min; BioTek Instruments).

Cellular TYR activity was determined by measuring the L-dopa oxidation rate. The cells were lysed with cell lysis buffer (containing 1% (*V/V*) PMSF), and total protein was extracted. Total protein content was quantified using the BCA protein assay kit (Beyotime Biotechnology). Then, 100 μL of PBS (pH 6.8) containing 20 μg of protein was mixed with 100 μL of 0.01% g/mL L-dopa and added to a 96-well plate. The mixture solution was then incubated at 37 °C for 1 h in the dark, and the absorbance was measured at 475 nm (BioTek Instruments).

2.10. Zebrafish experiment

Zebrafish embryos were cultured and selected from Science Research Centre in Tong Ren Hospital at the Shanghai Jiao Tong University School of Medicine (Shanghai, China). The detailed

procedure of the reproduction method is described in a previous study [9]. Zebrafish embryos were cultured in a 6-well plate and then treated with *N*-phenylthiourea (PTU; 200 μM) or co-treated with EB (0.5, 1, and 5 mM) for 54 h. Images were captured using a stereoscope (Olympus Corporation).

2.11. Mouse experiment

Per the rules of Laboratory Animal Care and International Law on Animal Experimentation (Rule Nos.: PZSHUTCM210305006 and PZSHUTCM211213002), all animal experiments were conducted in agreement with the protocols stipulated by the Faculty Animal Committee at the Shanghai University of Traditional Chinese Medicine. HQ (4%, *m/m*), monobenzone (40%, *m/m*), and EB (0.1% and 0.5%, *m/m*) were dissolved in an oil-in-water emulsion cream containing water (61.3%), stearic acid (8.0%), white vaseline (8.0%), glycerol (7.0%), octadecanol (6.0%), propylene glycol (5.0%), azone (2.0%), trolamine (1.6%), SDS (1.0%), and ethylparaben (0.1%). Male C57BL/6 mice (6 weeks old) were purchased from Charles River Laboratories Co., Ltd. (Shanghai, China). The mice were housed in a controlled environment of 12-h daylight schedule at a temperature of 23 ± 1 °C and 50% relative humidity, and food and water were supplied *ad libitum*.

2.11.1. Hydroquinone mouse model experiment

After adaptation to the environment for 1 week, mice were randomized to four groups: control group (received only emulsion cream), model group (received 4% (*m/m*) HQ for one half-day and emulsion cream for the other half-day), low-dose EB group (received 4% (*m/m*) HQ for one half-day and 0.1% (*m/m*) EB for the other half-day), and high-dose EB group (received 4% (*m/m*) HQ for one half-day and 0.5% (*m/m*) EB for the other half-day; the EB doses were decided according to a previous study [11]). Five mice were included in each group. Rosin and paraffin were used to remove hair at the back of the mice. All mice received the treatment for 50 days, and the body weight of mice was recorded every two days. Images were captured to observe hair color on days 1 and 50. Dorsal skin tissues were collected and stained with H&E, and TYR activity was measured (using the same method as that used for cellular TYR activity assay).

2.11.2. Monobenzone mouse model experiment

After adaptation to the environment for one week, mice were randomized to four groups: control group (received only emulsion cream), model group (received 40% (*m/m*) monobenzone for one half-day and emulsion cream for the other half-day), low-dose EB group (received 40% (*m/m*) monobenzone for one half-day and 0.1% (*m/m*) EB for the other half-day), and high-dose EB group (received 40% (*m/m*) monobenzone for one half-day and 0.5% (*m/m*) EB for the other half-day). Eight mice were included in each group. Hair was shaved at the back of mice. All mice received treatment for 54 days and were monitored daily until day 65. The body weight of mice was recorded every two days. Images were captured to observe hair color on days 1 and 65. Dorsal skin tissues were collected to measure TYR activity, performed quantitative RT-PCR assay, and stained with anti-TYR (Abcam Trading Co., Ltd.).

2.12. Cycloheximide chase assay

Cells were treated with CHX (25 μg/mL), which is a protein synthesis inhibitor, and cotreated with monobenzone (30 μM) and EB (100 μM) for 0, 6, 12, and 24 h. The cells were lysed with cell lysis buffer (containing 1% (*V/V*) PMSF), and total protein content was determined using the BCA Protein Assay kit (Beyotime

Biotechnology). The extracted protein was subjected to immuno-blotting to evaluate TYR, TYRP1, and DCT expression. The signals were visualized using Tanon 4600SF (Tanon Technology Co., Ltd.) and determined by quantitative analysis of digital images of gels using ImageJ (version 1.8.0).

2.13. Immunoprecipitation and co-immunoprecipitation assays

Cells were lysed with cell lysis buffer (containing 1% (*V/V*) PMSF), after which total protein was extracted, and its content was determined using the BCA Protein Assay kit (Beyotime Biotechnology). Protein A (5 μL) and Protein B (5 μL) beads were added to 500 μL of cell lysate (protein concentration: 2 mg/mL) and subjected to rotary incubation at 4 °C for 1 h to eliminate nonspecific protein (Absin Biotechnology Co., Ltd., Shanghai, China). The supernatant was collected, and anti-TYR (Abcam Trading Co., Ltd.), anti-TYRP1 (Abcam Trading Co., Ltd.), anti-DCT (Abcam Trading Co., Ltd.), and anti-IgG (Santa Cruz Biotechnology, Inc.) were added to the supernatant to precipitate the target protein, followed by rotary incubation at 4 °C overnight. Subsequently, Protein A (5 μL) and Protein B (5 μL) beads were added to the protein solution, followed by rotary incubation at 4 °C for 1 h. The sediment was collected and washed thrice with wash buffer and then subjected to immuno-blotting assay. Anti-calnexin (Santa Cruz Biotechnology, Inc.) and anti-ubiquitin (Santa Cruz Biotechnology, Inc.) were added to the immunoblot and incubated at 4 °C overnight, followed by probing with the corresponding secondary antibody at room temperature for 1 h. The signals were visualized using Tanon 4600SF (Tanon Technology Co., Ltd.).

2.14. Proximity ligation assay

Cells were cultured on coverslips in a 24-well plate and treated with monobenzone (60 μM) and EB (100 μM) for 6 h. The cell supernatant was discarded, and the cells were washed thrice with PBS, after which they were fixed in 4% paraformaldehyde for 10 min and treated with 0.1% (*V/V*) Triton for 5 min. The cells were incubated with anti-TYR (Abcam Trading Co., Ltd.), anti-TYRP1 (Abcam Trading Co., Ltd.), and anti-calnexin (Santa Cruz Biotechnology, Inc.). The other reagents and procedures refer to the Duolink Proximity Ligation Assay (Sigma-Aldrich), and the procedure was performed according to the manufacturer's instructions. Images were captured using a confocal microscope (SP8; Leica), and signals were determined by quantitative analysis using ImageJ (version 1.8.0).

2.15. Statistical analysis

Statistical analysis was performed using GraphPad Prism 8.0 software (UK), and data were expressed as mean $\pm$ standard error of the mean. Multiple groups were analyzed using a one-way analysis of variance, followed by the Dunnett *t*-test. Both groups were analyzed using unpaired two-tailed *t*-tests. $P < 0.05$, $P < 0.01$, and $P < 0.001$ were considered to be statistically significant.

3. Results

3.1. Epimedin B increases melanin production

The main bioactive constituents in the *Epimedium brevicornum* Maxim. extract were identified using high performance liquid chromatography (HPLC). EB (Figs. 1A and B) showed the highest effect on melanogenesis and TYR activation (Fig. S1; for more details, refer to our previous study [8]). To verify the melanogenic effect, the melanin content in both melanoma cell lines
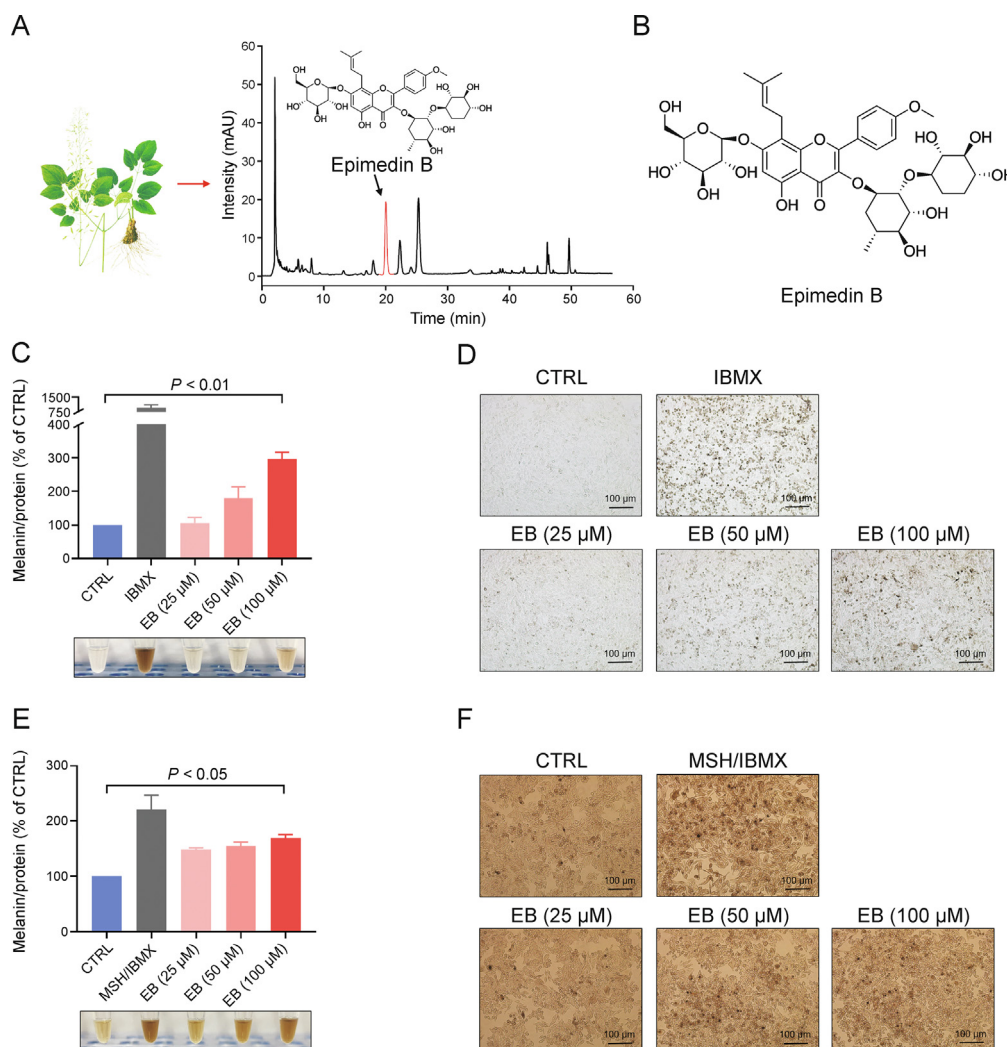
Fig. 1. Epimedin B (EB) increases melanin production in a concentration- and time-dependent manner. (A) EB is a main bioactive constitute in *Epimedium brevicornum* Maxim. extract identified by using high-performance liquid chromatography (HPLC). (B) The structure of EB (PubChem CID: 5748393). (C) Melanin contents, melanin color on B16F10 cells based on different concentration of 25, 50, and 100 μM for 72 h, isobutylmethylxanthine (IBMX) (100 μM). (D) Representative images of intracellular melanin granules on B16F10 cells. (E) Melanin contents, melanin color on MNT-1 cells based on different concentration of 25, 50, and 100 μM for 72 h, IBMX (100 μM), α-melanocyte-stimulating hormone (α-MSH) (100 nM). (F) Representative images of intracellular melanin granules on MNT-1 cells. For graphical representation, data are presented as mean ± standard error of the mean ($n \geq 3$ in each group). $P < 0.05$ and $P < 0.01$ vs. control (CTRL) are considered to be significant. Representative image from three independent experiments is shown.

(B16F10 cells and MNT-1 cells) obtained from different species was determined by treating with different concentrations of EB (25, 50, and 100 μM) for 72 h (cell viability assay was performed in our previous study [8]). IBMX, a cAMP-elevating agonist for melanogenesis, and α-MSH were used as a positive control. In B16F10 cells, the intracellular melanin content significantly increased in a dose-dependent manner, particularly showing a nearly threefold increase with the highest concentration of EB. The dissolved melanin in the microtube appeared visibly darkened (Fig. 1C). Consistently, photos of intracellular substances confirmed more pigment generation with an increase in the EB dose (Fig. 1D). Similarly, the increase in the melanogenic effect and melanin content in MNT-1 cells was observed with an increase in the EB dose (Figs. 1E and F).

To evaluate whether EB-induced melanogenesis occurred in a time-dependent manner, melanin content was examined at different time points (0, 12, 24, 48, and 72 h). As expected, the melanin content evidently increased in a time-dependent manner in both cell lines. Notably, the melanin content showed a sharp increase until 72 h in B16F10 cells (Figs. 2A and B). By contrast, the

melanin content in MNT-1 cells showed a stable increasing trend (Figs. 2C and D). The reason for this result was that MNT-1 cells are a type of highly pigmented melanoma cells, and the preliminary melanin content in MNT-1 cells is more than that in B16F10 cells.

To sum up, our results indicate that EB exhibits melanogenic effects in both melanoma cells *in vitro*, and 72-h treatment with the 100 μM dose of EB was selected for subsequent experiments.

3.2. Epimedin B promotes melanosome biosynthesis

To further validate the melanogenic effect of EB, human skin tissue samples were collected and examined. When treated with EB (100 μM) for 72 h, purified human primary melanocytes produced and secreted more melanin granules as observed under a phase-contrast microscope (Fig. 3A). Next, we tested EB on healthy human donors' skin explant culture. Histology analysis with Fontana-Masson staining (a melanin-specific dye) showed an increase in melanin signals at the junction of the epidermis and dermis after EB (1 mM) treatment for a week (Fig. 3B). Postinflammatory depigmentation indicated acquired partial and total loss of skin
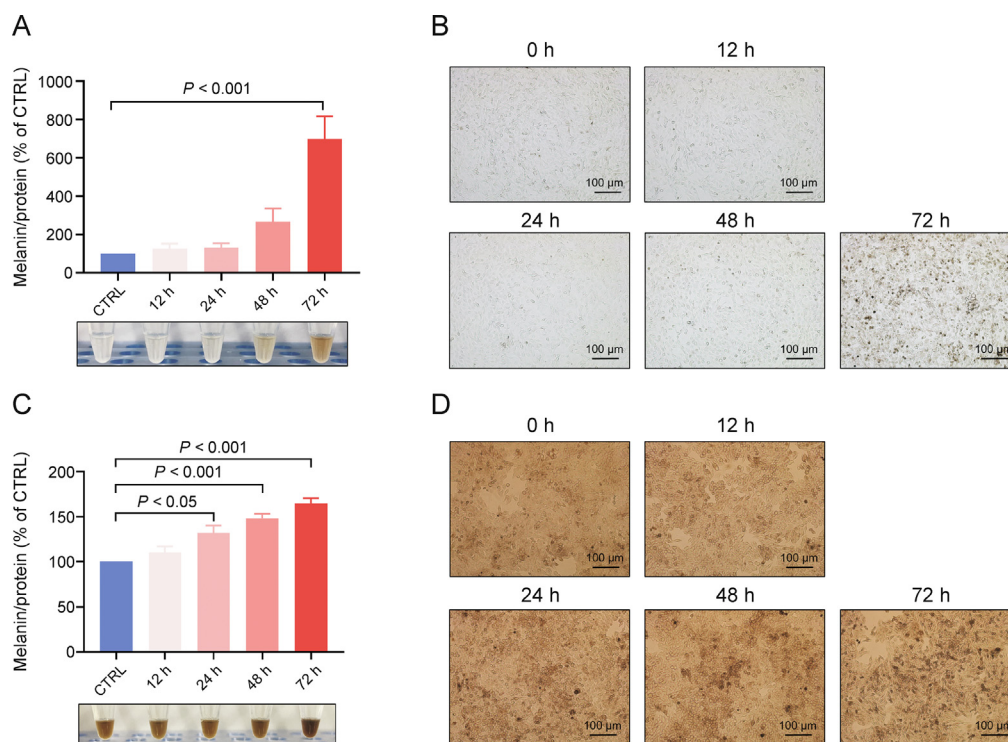
Fig. 2. Epimedin B (EB) increases melanin production in a concentration- and time-dependent manner. (A) Melanin contents, melanin color on B16F10 cells based on different time of 12, 24, 48, and 72 h by EB (100 μM). (B) Representative images of intracellular melanin granules on B16F10 cells. (C) Melanin contents, melanin color on MNT-1 cells based on different time of 12, 24, 48, and 72 h by EB (100 μM). (D) Representative images of intracellular melanin granules on MNT-1 cells. For graphical representation, data are presented as mean ± standard error of the mean ($n \geq 3$ in each group). $P < 0.05$, $P < 0.01$, and $P < 0.001$ vs. control (CTRL) are considered to be significant. Representative image from three independent experiments is shown.

pigmentation. We collected tissues from donors with depigmented lesions and cultured the tissues with EB (1 mM) for a week. Immunohistochemistry staining with HMB45 (a melanosome marker) showed that more positive signals were generated around the nucleus at the basal epidermal level in the treated tissues than in untreated control tissues (Fig. 3C). Collectively, our data demonstrated a significant melanogenic effect induced by EB in primary melanocytes, human skin organ culture, indicating that this phenotype was achieved by regulating melanosomes.

Melanosomes are subcellular lysosome-like organelles in which the melanin pigment is synthesized and stored before distribution to the surrounding keratinocytes [2]. Melanosome number, size, and maturation stage reflect the melanogenic ability of melanocytes. Thus, it is necessary to investigate the changes in melanosomes under the EB-induced pigmentation phenotype. Immunofluorescence confocal microscopy analysis suggested that more number of melanosomes (observed after staining with HMB45) was present in the EB treatment group than in the control group (Fig. 3D). Notably, melanosomes in the EB and IBMX groups (positive control) were distributed from the nucleus to the cellular periphery; however, melanosomes in the control group were located around the nucleus (Fig. 3D), indicating that EB increases melanosome number and regulates intramelanocytic melanosome distribution. As shown previously, only mature melanosomes could be transferred to the periphery of melanocytes, while immature melanosomes aggregated around the perinuclear region, which was their point of origin [2]. We then detected melanosome stage by transmission electron microscopy analysis. Ultrastructure analysis of melanosomes revealed that EB stimulation was the driving factor for the striking increase in late-stage/pigmented melanosomes (stage III and IV melanosomes) (Fig. 3E), whereas melanosomes in the control group had early-stage/unpigmented

melanosomes (stage I and II melanosomes; Fig. 3E). These findings suggest that EB stimulates melanin biosynthesis by increasing melanosome number and driving melanosome maturation. Furthermore, we performed a global transcriptional analysis of human primary melanocytes and identified 361 differentially expressed genes ($P < 0.05$) between the untreated and EB-treated melanocytes that were enriched in seven sectors of biological process wherein the process of "pigment melanin secondary biosynthetic" was involved (Figs. 3F and G). The process of "Pigment melanin secondary biosynthetic" comprised various biological processes and cellular components including "Melanin biosynthetic process," "Melanosome/melanosome membrane," etc. (Fig. 3H). These data confirm the regulatory role of EB in melanin biosynthesis and melanosome formation.

3.3. Epimedin B increases TYRs expression

Melanosomes require several specific enzymatic and structural proteins to mature and become adequately competent to produce melanin [1]. In mammals, such enzymatic proteins encoded by specific-melanocyte gene products act to coordinate the tightly regulated melanogenesis pathway. Moreover, transcriptional data of human primary melanocytes indicated that multiple melanogenesis-related biological processes were notably regulated by EB treatment (Figs. 3F−H). To elucidate the mechanism underlying EB-induced melanogenesis, we investigated the participation of TYRs. In human primary melanocytes, the fluorescence intensity of TYR was significantly enhanced in the EB group (Fig. 4A). Additionally, Western blotting analysis showed that TYR, TYRP1, and DCT expression was upregulated remarkably in B16F10 melanoma cells treated with EB (100 μM; Figs. 4B and C). In line with melanosome data (Figs. 3D and E), EB treatment (100 μM) evidently
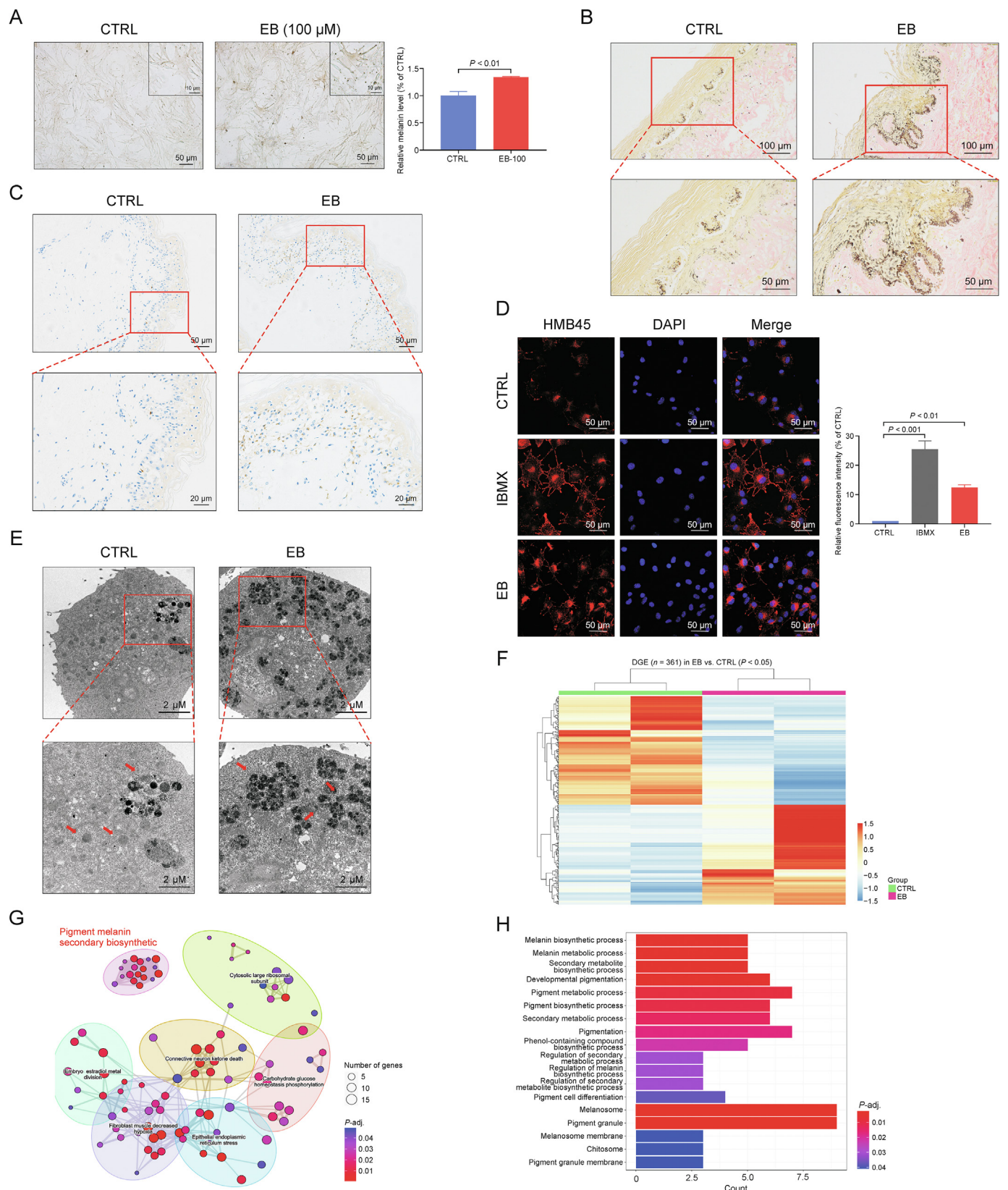
Fig. 3. Epimedin B (EB) promotes melanin biosynthesis by increasing melanosome number and maturation. (A) Representative images of human primary melanocytes under phase contrast microscope, and relative melanin contents statistics. (B) Representative images of healthy human skin tissue for Masson-Fontana staining. (C) Representative images of lesion tissues area of depigmented donors for immunohistochemistry staining (nucleus: blue; melanin granules: brown black). (D) Representative images of immunofluorescence staining on B16F10 cells (red: HMB45 (referred to as melanoma gp100), blue: 4′,6-diamidino-2-phenylindole (DAPI); isobutylmethylxanthine (IBMX): 100 μM, EB: 100 μM treated for 72 h); and fluorescence intensity statistics for HMB45. (E) Representative images of melanosome in B16F10 cell using transmission electron microscopy. (F) Heat map of 361 differential genes between control (CTRL) and EB groups; differential genes expression (DGE). (G) 361 differential genes were enriched in seven sectors of biological processes:
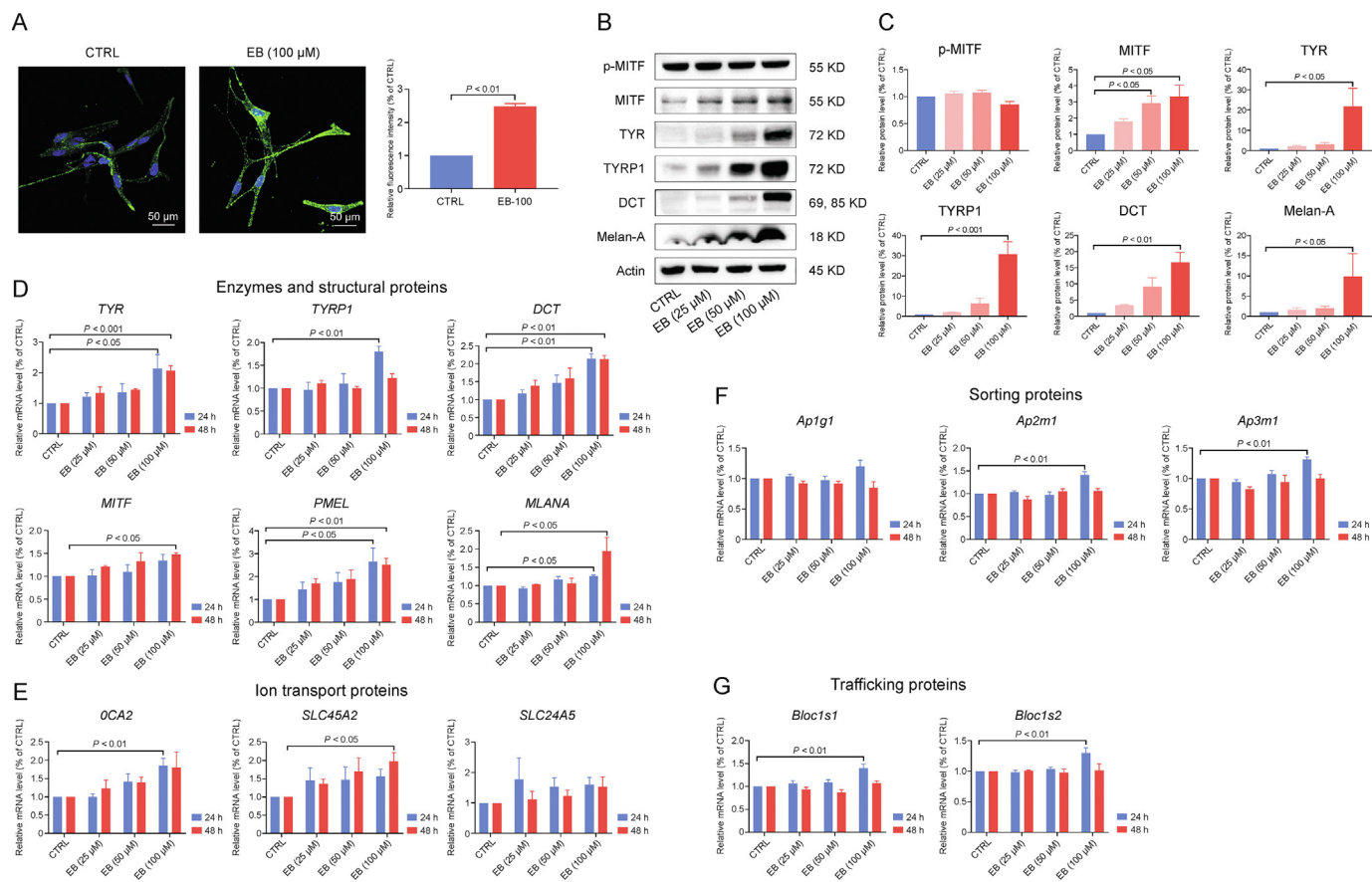
Fig. 4. Epimedin B (EB) increases tyrosinase family of proteins (TYRs) expression through microphthalmia-associated transcription factor (MITF)-mediated p-AKT (referred to as protein kinase B (PKB))/glycogen synthase kinase 3β (GSK3β)/β-catenin, p-p70 S6 kinase cascades, and protein 38 (p38)/mitogen-activated protein (MAP) kinase (MAPK) and extracellular regulated protein kinases (ERK)/MAPK pathways. (A) Representative images of immunofluorescence staining on primary human melanocytes (green: tyrosinase (TYR), blue: 4′,6-diamidino-2-phenylindole (DAPI); EB: 100 μM treated for 72 h), and fluorescence intensity statistics for TYR. (B) The protein expression levels of p-MITF, MITF, TYR, TYR-related protein 1 (TYRP1), dopachrome tautomerase (DCT), and melanoma antigen (Melan-A) (72 h on B16F10 cells). (C) Relative protein levels for p-MITF, MITF, TYR, TYRP1, DCT, and Melan-A expression. (D) The messenger RNA (mRNA) expression levels of *TYR*, *TYRP1*, *DCT*, *MITF*, premelanosome protein (*PMEL*), and Melan-A (*MLANA*) on B16F10 cells. (E) The mRNA expression levels of *OCA2*, *SLC45A2*, and *SLC24A5* on B16F10 cells. (F) The mRNA expression levels of *Ap1g1*, *Ap2m1*, and *Ap3m1* on B16F10 cells. (G) The mRNA expression levels of *Bloc1s1* and *Bloc1s2* on B16F10 cells. For graphical representation, data are presented as mean ± standard error of the mean ($n \geq 3$ in each group). $P < 0.05$, $P < 0.01$, and $P < 0.001$ vs. control (CTRL) are considered to be significant. Representative image from 3 independent experiments is shown.

increased Melan-A expression in B16F10 melanoma cells (Figs. 4B and C). In addition to the protein expression level, the messenger RNA (mRNA) expression of *TYR*, *TYRP1*, *DCT*, premelanosome protein (*PMEL*), and Melan-A (*MLANA*) (encoding melanosome structural proteins) was upregulated by EB both at 24 h and at 48 h (Fig. 4D), suggesting the EB-induced dual positive regulation of TYRs at the mRNA and protein levels. MITF is a well-known pivotal regulator of TYRs and a master regulator of melanogenesis. MITF not only is regulated at the transcriptional level but also undergoes different post-transcriptional modifications that affect MITF transcriptional activity [1]. We detected MITF expression and its common phosphorylation form and reported that the mRNA and protein expression levels of MITF were significantly upregulated by EB stimulation, but no change was observed in p-MITF (Figs. 4B–D). These findings suggest that EB upregulated TYRs expression in melanogenesis through the classic MITF-dependent mechanism.

Only the new synthetic TYRs are transferred from the Golgi apparatus to melanosomes, and being located in the melanosome

membrane, they exert enzymatic functions. Multiple functional proteins encoded by melanocytic genes, including ion transport proteins (*OCA2*, *SLC45A2*, and *SLC24A5*), membrane-associated sorting proteins (*Ap1g1*, *Ap2m1*, and *Ap3m1*), tubule-dependent trafficking proteins (*Bloc1s1* and *Bloc1s2*), are involved in melanosome biogenesis by sorting cargo proteins, forming transported tubules, and controlling the melanosomal lumen environment, wherein TYRs catalyze melanin production [12]. EB can affect the mRNA expression of these genes, especially *OCA2* and *SLC45A2* at 24 or 48 h (Figs. 4E–G), suggesting the sophisticated processes regulated by EB in melanosome biogenesis and maturation, which may account for the changes in increased melanosome number and melanin content in melanosomes.

Mature melanosomes are then transferred from melanocytes to keratinocytes, and melanocyte dendrites are considered as important transfer channels [3]. We quantified the mRNA and protein expression levels of Rab27a, RhoA, and CDC42 (responsible for dendrite growth) but found no significant changes in EB-treated

"Pigment melanin secondary biosynthetic", "Cytosolic large ribosomal subunit", "Embryo estradiol metal division", "Connective neuron ketone death", "Carbohydrate glucose homeostasis phosphorylation", "Fibroblast muscle decreased hypoxia", and "Epithelial endoplasmic reticulum stress". (H) The "Pigment melanin secondary biosynthetic" comprised by 18 kinds of biological processes and cellular components. For graphical representation, data are presented as mean ± standard error of the mean ($n = 2$ in transcriptome data; $n \geq 3$ in other each group), $P < 0.05$, $P < 0.01$, and $P < 0.001$ vs. CTRL are considered to be significant. Representative image from three independent experiments is shown.

B16F10 melanoma cells (Figs. S2A–C). As for the morphology of cell dendrites/tips, there was no development of outgrowth/extension as observed on staining with phalloidin (a cytoskeleton marker; Fig. S2D). These data confirm that EB has a lesser effect on melanosome transfer between melanocytes and keratinocytes.

Melanin production is initiated and regulated by several signaling systems [1]. To clarify the upstream mechanism underlying melanogenesis after EB treatment, we investigated the effect of EB on melanogenic signaling pathways (Fig. 5A). The cAMP level and PKA expression were unaffected by EB (Fig. 5B and C), indicating that the classic cAMP-PKA-MITF pigmentation pathway was not involved in EB-induced melanogenesis. By contrast, the cascade of the PI3K/AKT signaling pathway was affected, including GSK3β/β-catenin and p-p70 S6 kinase (Figs. 5B and C). Mitogen-activated protein (MAP) kinase (MAPK) pathway is well known to regulate melanogenesis [1,13,14]. We investigated the molecules present downstream of the MAPK signaling cascade, including p38, JNK, ERK, and their phosphorylated form. Western blotting analysis showed that p-p38 and p-ERK expression was downregulated and

upregulated, respectively, having no influence on p-JNK after EB stimulation (Figs. 5B and C). These data prove that EB exerts control of multiple pigment pathways to affect melanin production.

3.4. Epimedin B promotes TYR activity

In melanin synthesis, TYR is the pivotal enzyme that catalyzes the rate-limiting step (hydroxylation of L-tyrosine to L-dopa). To explore the effect of EB on TYR catalytic activity, we first tested the reaction rate of mushroom TYR and the substrate L-dopa by simultaneously adding EB. The Michaelis constant (K_m) of 50 and 100 μM EB (K_m: 1.387 and 1.909) were lower than the control K_m values (K_m: 2.043; Fig. 6A), suggesting that EB can accelerate the reaction rate of mushroom TYR and the substrate L-dopa. Furthermore, the effect of EB on mammalian TYR activity was determined in two melanoma cells. Coincident with the melanogenic effect (Figs. 1C–F), TYR activity was significantly enhanced with 100 μM EB in a dose-dependent manner in B16F10 and MNT-1 melanoma cells (Figs. 6B and C, left panel). Interestingly,
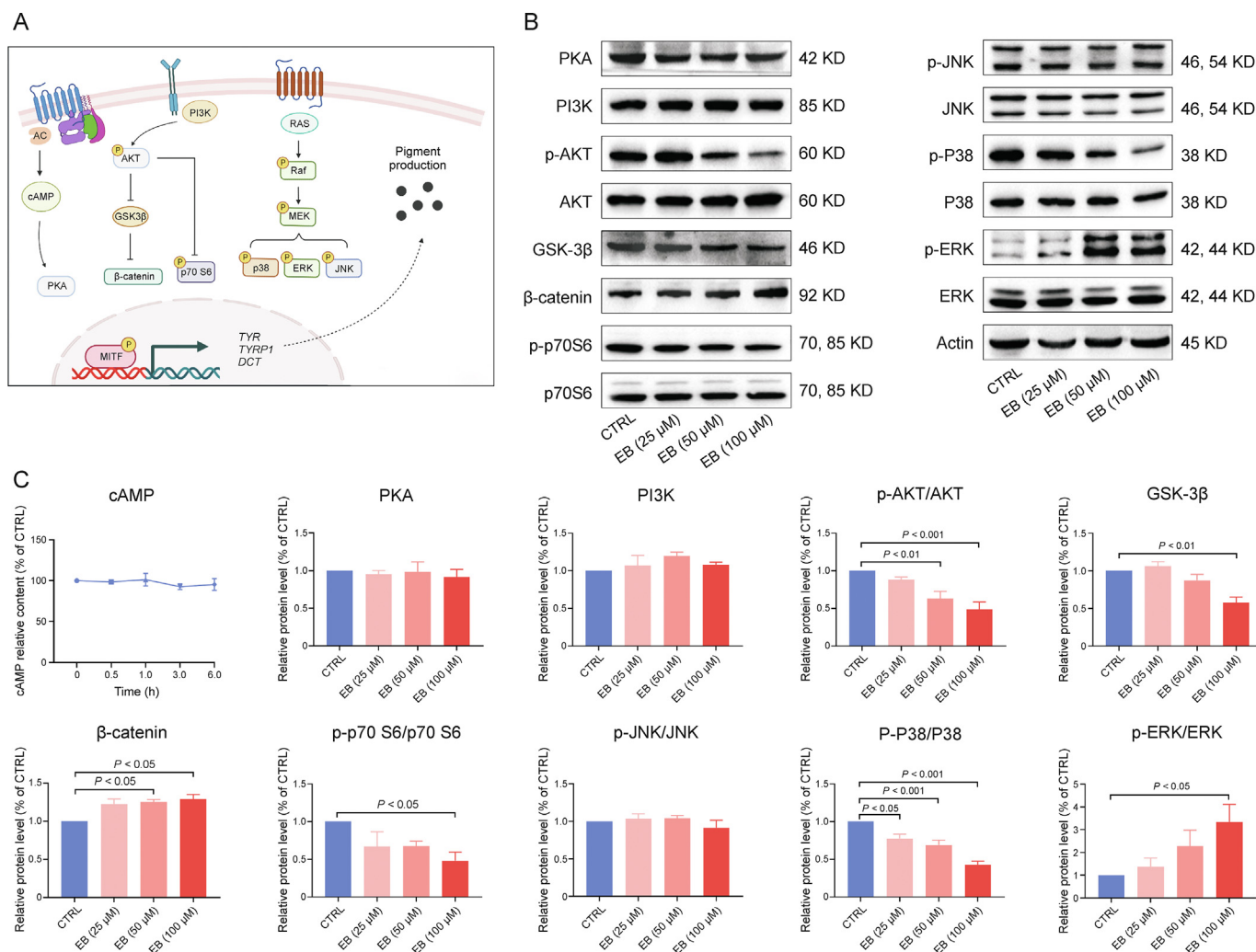
Fig. 5. Epimedin B (EB) increases tyrosinase family of proteins (TYRs) expression through microphthalmia-associated transcription factor (MITF)-mediated p-AKT (referred to as protein kinase B (PKB))/glycogen synthase kinase 3β (GSK3β)/β-catenin, p-p70 S6 kinase cascades, and protein 38 (p38)/mitogen-activated protein (MAP) kinase (MAPK) and extracellular regulated protein kinases (ERK)/MAPK pathways. (A) Diagram of signal pathways in melanogenesis: adenylyl cyclase (AC), rat sarcoma (RAS), Raf protein kinase (Raf), and MAP kinase (MEK). (B) The protein expression levels of protein kinase A (PKA), phosphoinositide 3-kinase (PI3K), p-AKT, AKT, GSK-3β, β-catenin, p-p70 S6, p70 S6, p-c-Jun N-terminal kinase (JNK), JNK, p-p38, p38, p-ERK, and ERK (24 h on B16F10 cells). (C) Statistics for cellular cyclic AMP (cAMP) contents for 0, 0.5, 1, 3, and 6 h; PKA, PI3K, p-AKT, AKT, GSK-3β, β-catenin, p-p70 S6, p70 S6, p-JNK, JNK, p-p38, p38, p-ERK, and ERK expression. For graphical representation, data are presented as mean ± standard error of the mean ($n \geq 3$ in each group). $P < 0.05$, $P < 0.01$, and $P < 0.001$ vs. control (CTRL) are considered to be significant. TYRP1: TYR-related protein 1; DCT: dopachrome tautomerase.
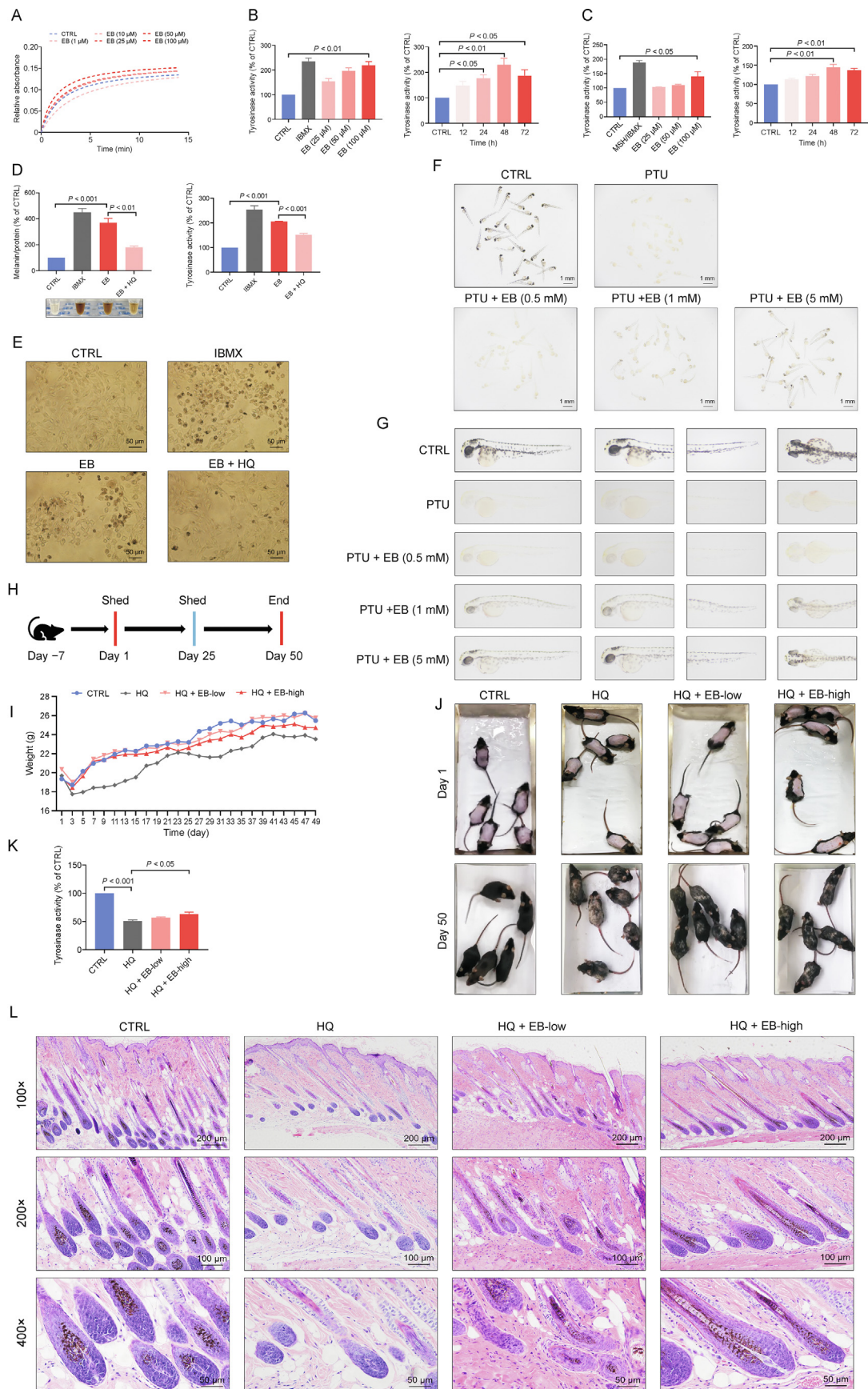
intracellular TYR activity peaked at 48 h in both melanoma cells (Figs. 6B and C, right panel), whereas the highest melanin content was observed at 72 h (Fig. 2). HQ, which is a well-known TYR inhibitor, was selected to confirm EB-induced melanogenesis through enhanced TYR activity. EB-induced melanogenesis and TYR activity were effectively inhibited after treatment with HQ, which emphasizes the melanogenic effect of EB through TYR activation (Figs. 6D and E).

To determine whether EB can serve as a TYR activator and can exert a repigmentation effect *in vivo*, we developed two models of depigmentation, in zebrafish and mice, with TYR inhibitors. The depigmented model of zebrafish was induced by PTU, a frequently-used TYR inhibitor. PTU-caused depigmented zebrafish showed evident repigmentation through a reversal effect after co-treatment with EB at a relatively high dose (Figs. 6F and G). HQ is also often used as a depigmenting agent because its structure is similar to tyrosine [15]. Thus, we treated EB to the back skin of C57BL/6 mice to evaluate its interference with melanogenesis. After 50 days (near two follicle cycles), mice in the control group had black hair. The only HQ-treated group had mass hair graying at the back of mice. Mice that received co-treatment with EB (0.1% and 0.5%) had an evident blockade of HQ-induced gray hair formation (Figs. 6H and J). H&E staining of the follicle section co-confirmed more pigment content within the hair bulge and shaft during the anagen stage in the treatment group than in the model group (Fig. 6L). The lack of evident differences in body weight implied percutaneous safety (Fig. 6I). Mouse dorsal skin tissues were collected and determined for TYR activity. The results showed that high-dose EB effectively reactivated cutaneous TYR activity in the HQ-caused depigmented model (no significant difference, but with a reactivation effect at a low dose; Fig. 6K).

Collectively, our data suggest that EB exerts pigmentation by promoting TYR activity *in vitro* and *in vivo*.

3.5. Epimedin B increases melanin content and TYRs expression against monobenzone-induced depigmentation

Early studies on TYR stability revealed that TYR is degraded endogenously in melanoma cells. Equal to its synthesis, TYR degradation is tightly connected to its function and is an important parameter for melanogenesis [6]. Monobenzone is a local depigmentation agent that is used for treating over-pigmentation in the clinic setting. In healthy users, monobenzone can induce vitiligo-like depigmentation through the TYR and melanosome degradation mechanism [15,16]. Thus, we used monobenzone to investigate whether EB exertes a repigmentation effect and affects TYRs and melanosome abnormal degradation. Cell viability test results proved that treatment with 5 μM monobenzone for 72 h caused no harmful effects in B16F10 cells and MNT-1 cells (data not shown). In melanin production, monobenzone effectively decreased melanin content, especially in B16F10 melanoma cells (Figs. 7A and B). As expected, EB significantly ameliorated monobenzone-induced melanogenesis dysfunction in both melanoma cells (Figs. 7A and B). A similar repigmentation effect was confirmed in human primary melanocytes, even though the

melanin content in these cells is not as much as that in melanoma cells (Fig. 7C). Moreover, we incubated healthy donors' skin tissue with monobenzone (60 μM) and EB (1 mM) for a week. Immunofluorescence staining analysis showed that monobenzone notably decreased histological TYR and melanosome expression in the entire top layer of the dermis in the treatment group compared with those in the control group (Fig. 7D). EB treatment provided effective protection against monobenzone-induced reduction of TYR and melanosome in cultured skin tissues (Fig. 7D). We also quantified intracellular TYRs and melanosome expression level after treatment with monobenzone and EB. Western blotting analysis showed that the protein expression of TYR, TYRP1, DCT and Melan-A was reduced after monobenzone treatment (Figs. 7E and F). During co-treatment with monobenzone and EB, the expression of TYRs and Melan-A was markedly upregulated (Figs. 7E and F). Notably, monobenzone-induced inhibition of melanogenesis and reduction of TYRs expression were not dependent on TYR activity inhibition (Fig. 7G) or on the decline of *MITF*, *TYR*, *TYRP1*, and *DCT* mRNA expression levels, including even the modest increase in *TYR* mRNA expression for 24 h (Fig. 7H).

Our data indicate that EB can protect melanin and TYRs against monobenzone-induced depigmentation.

3.6. Epimedin B improves TYR and TYRP1 stability

Monobenzone causes TYR degradation without affecting TYRs transcriptional levels. To investigate whether EB has influence on TYRs stability, we used CHX to inhibit protein synthesis for excluding EB, by itself, induced new synthetic TYRs. Western blotting analysis showed that monobenzone significantly decreased TYRs stability, which was effectively prevented by EB treatment (Fig. 8A), indicating that EB significantly improved monobenzone-induced TYRs stability rather than merely improving it by enhancing transcriptional ability.

Although the mechanism of TYRs degradation is not fully understood, researches on glycosylation of TYRs disclosed that degradation event of TYR in ER is proteolyzed by ubiquitin-proteasome through the ERAD pathway [6]. Thus, we hypothesized that EB function might be associated with the ubiquitin-proteasome pathway. Immunoprecipitation analysis showed that notable ubiquitination was increased on purified TYRs after treatment with 60 μM monobenzone for 6 h (Figs. 8B and S3A), and ubiquitination of aberrant TYR and TYRP1 (approximately 60 kDa) was prevented after co-treatment with 100 μM EB (Fig. 8B). However, reduction of ubiquitination of aberrant DCT was not observed around the 55–43 kDa site after co-treatment with 100 μM EB (Fig. S3A). Monobenzone-induced enhanced expression of abnormal-molecular-mass TYRs tagged with ubiquitin and monobenzone-induced alleviation of the expression of abnormal-molecular-mass TYRs after EB co-treatment inspired us to investigate whether EB affects TYRs' maturation process to control their quality. In this process, molecular chaperones in the ER, which assist protein maturation, play an important role in the retention of misfolded proteins in the ER [6]. Hence, to investigate the effect

---

Fig. 6. Epimedin B (EB) promotes tyrosinase (TYR) activity to exert a pigmentation effect. (A) Mushroom TYR activity assay (EB: 1, 10, 25, 50, and 100 μM). (B) TYR activity on B16F10 cells based on different concentration of 25, 50, and 100 μM for 72 h, isobutylmethylxanthine (IBMX) (100 μM), and different time of 12, 24, 48 and 72 h by EB-100 μM. (C) TYR activity on MNT-1 cells based on different concentration of 25, 50, and 100 μM for 72 h, IBMX (100 μM), α-melanocyte-stimulating hormone (α-MSH) (100 nM), and different time of 12, 24, 48, and 72 h by EB (100 μM). (D) Melanin contents, melanin color, and TYR activity on B16F10 cells for 72 h (IBMX: 100 μM; EB: 100 μM; hydroquinone (HQ): 25 μM). (E) Representative images of intracellular melanin granules on B16F10 cells. (F) Images of melanin in general zebrafishes (*N*-phenylthiourea (PTU): 200 μM; EB: 0.5, 1, and 5 mM). (G) Representative images of melanin in zebrafish. (H) Timeline of mice experiment procedure. (I) Statistic for mice bodyweight. (J) Images of C57BL/6 mice dorsal hair color. (K) TYR activity of mice dorsal skin. (L) Representative images of hematoxylin eosin staining of mice hair follicle. For graphical representation, data are presented as mean ± standard error of the mean ($n \geq 3$ in each group). $P < 0.05$, $P < 0.01$, and $P < 0.001$ vs. control (CTRL) are considered to be significant. Representative image from three independent experiments is shown.
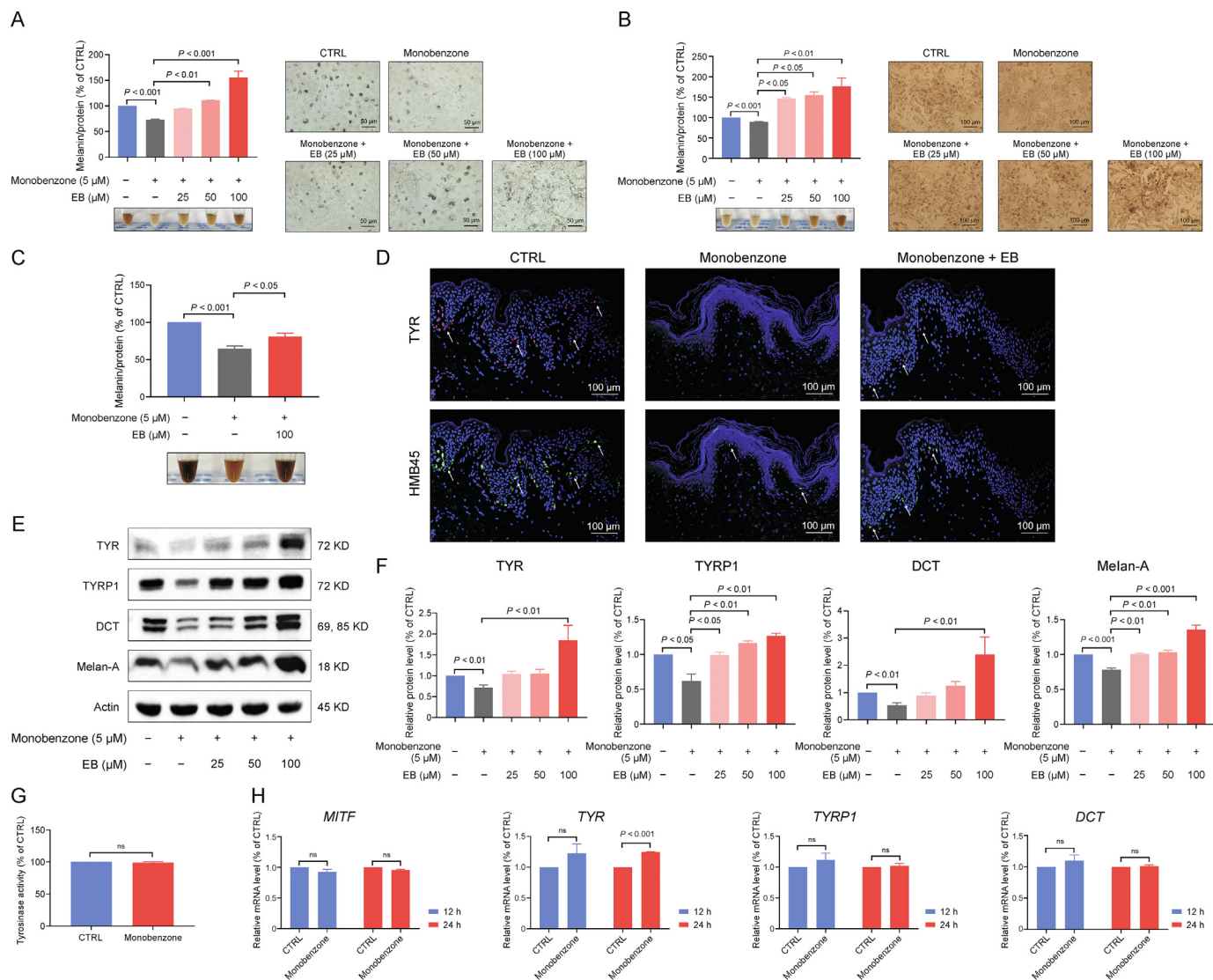
Fig. 7. Epimedin B (EB) increases melanin content and tyrosinase family of proteins (TYRs) expression against monobenzone-induced depigmentation. (A) Melanin contents and melanin color on B16F10 cells based on different concentration of EB (25, 50, and 100 μM) for 72 h, monobenzone (5 μM), and representative images of intracellular melanin granules on B16F10 cells. (B) Melanin contents and melanin color on MNT-1 cells based on different concentration of EB (25, 50, and 100 μM) for 72 h, monobenzone (5 μM), and representative images of intracellular melanin granules on MNT-1 cells. (C) Melanin contents, melanin color on primary human melanocytes (EB: 100 μM, monobenzone: 5 μM for 72 h). (D) Representative images of immunofluorescence staining in healthy human skin (red: tyrosinase (TYR), green: HMB45 (referred to as melanoma gp100), blue: 4′,6-diamidino-2-phenylindole (DAPI); monobenzone: 60 μM, EB: 1 mM treated for one week). (E) The protein expression levels of TYR, TYR-related protein 1 (TYRP1), dopachrome tautomerase (DCT), and melanoma antigen (Melan-A) on B16F10 cells (monobenzone: 5 μM, EB: 25, 50, and 100 μM treated for 72 h). (F) Statistics for TYR, TYRP1, DCT, and Melan-A expression. (G) TYR activity on B16F10 cells (monobenzone: 5 μM). (H) The messenger RNA (mRNA) expression levels of *TYR*, *TYRP1*, *DCT*, and microphthalmia-associated transcription factor (*MITF*) on B16F10 cells (monobenzone: 5 μM). For graphical representation, data are presented as mean ± standard error of the mean ($n \geq 3$ in each group). $P < 0.05$, $P < 0.01$, and $P < 0.001$ vs. control (CTRL) are considered to be significant. Representative image from 3 independent experiments is shown.

of EB on the generation of misfolded TYRs, we detected the calnexin (a molecular chaperone in the ER) content through co-immunoprecipitation experiments. Consistent with ubiquitination results, more aberrant TYRs-calnexin complexes were formed and captured after treatment with 60 μM monobenzone for 6 h (Figs. 8C and S3B). During co-treatment with EB, the formation of the TYR-calnexin complex and the TYRP1-calnexin complex effectively decreased, but the formation of the DCT-calnexin complex did not occur (Figs. 8C and S3B). To further confirm the formation of the TYR- and TYRP1-calnexin complexes, the precise simultaneous distribution and quantity were detected through the proximity ligation assay. Fluorescence assay results showed positive signals of TYR- and TYRP1-calnexin complexes were concentrated around the nucleus (location of the ER), with high intensity

in the monobenzone-treated group and low density in the EB co-treatment group (Figs. 8D and S3C). These data suggest that EB can decrease monobenzone-induced aberrant TYR and TYRP1 formation and enhance TYR and TYRP1 stability to lessen their ubiquitination.

Once the TYR-calnexin complex has formed, inhibition of α-glucosidase II prevents TYR from being released spontaneously from the complex, which results in TYR misfolding and accumulation in the ER. The misfolded proteins are tagged with ubiquitin labels, which play an important role as a sorting determinant for proteasomal degradation [6,17]. We double-stained B16F10 melanoma cells with calnexin as an ER marker and TYR to observe the expression and co-distribution in the ER. Confocal microscopy analysis showed that monobenzone treatment led to a decrease in
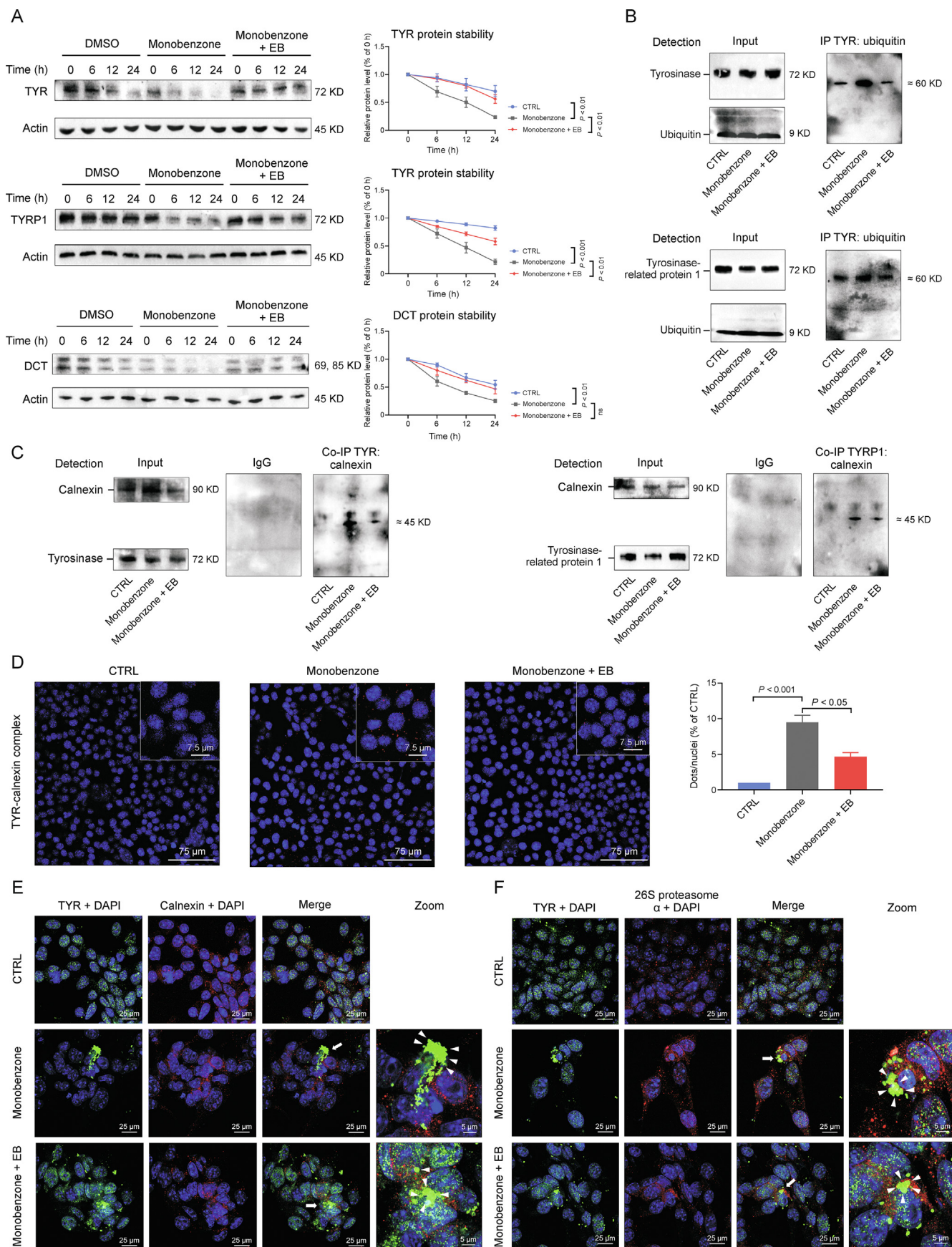
cellular TYR expression and granular accumulation of TYR in the ER when compared with mass and uniform TYR distribution in the control group (Fig. 8E). Co-treatment of monobenzone and EB effectively ameliorated TYR content and led to a scattered distribution, thereby preventing TYR congregation (Fig. 8E). A similar effect was observed in the double-stained TYRP1-calnexin assay in B16F10 melanoma cells (Fig. S3D). Furthermore, fluorescence colocalization analysis was performed to investigate the participation of the cellular proteasome in TYR and TYRP1 degradation by co-staining with 26S proteasome α (a proteasome marker). In contrast to monobenzone treatment, EB treatment decreased the overlapped fluorescence regions of 26S proteasome α and TYR (Fig. 8F), proving that fewer TYRs were degraded by proteasomes. As expected, double fluorescent staining of 26S proteasome α and TYRP1 showed the same results (Fig. S3E).

Collectively, these data suggest that EB improves TYR, TYRP1 stability by preventing monobenzone-induced aberrant TYR, TYRP1 formation, retention in the ER, and enhancement of the ubiquitin-proteasome degradation system.

3.7. Epimedin B ameliorates monobenzone-induced depigmentation in C57BL/6 mice

To investigate whether EB has repigmentation function in monobenzone-treated mice *in vivo*, we developed a 40% monobenzone-induced depigmented model and simultaneously treated the mice with EB based on previous studies [18,19]. Monobenzone and EB co-treatment was applied at the back of C57BL/6 mice for 54 days, and they were observed until day 65 (Fig. 9A). The results of mouse dorsal hair analysis showed that monobenzone-treated mice developed noticeable depigmentation in the application area (Fig. 9B). Mice co-treated with monobenzone and EB clearly ameliorated depigmented dorsal hair formation to varying degrees, which was particularly visible for the high-dose EB group (0.5%; Fig. 9B). Body weight data showed that 40% monobenzone treatment to mice can cause severe weight loss, especially during days 3–15 (Fig. 9C). This is perhaps attributed to severe inflammation with a massive exudate on the monobenzone-exposed sites. The dorsal skin tissues of the treated mice were collected, and cutaneous TYR activity was determined. The results showed that monobenzone had an inhibitory effect on cutaneous TYR activity (Fig. 9D), which was not found in melanoma cells *in vitro* (Fig. 7G). Co-treatment with EB could promote cutaneous TYR activity, which is significant for the high-dose EB group when compared with that for the monobenzone group (Fig. 9D). In addition, the mRNA levels of *TYR*, *TYRP1*, *DCT*, and *PMEL* were confirmed to be unaffected by monobenzone (Fig. 9E), emphasizing monobenzone-induced depigmentation independent of transcriptional regulation. Simultaneously, EB increased the mRNA expression of cutaneous *TYR*, *TYRP1*, *DCT*, and *PMEL* (Fig. 9E). We also stained the mouse hair follicle with TYR antibody and evaluated TYR expression mainly in the follicle bulges; TYR expression evidently decreased with monobenzone treatment and increased with EB co-treatment (Fig. 9F).

Thus, EB can ameliorate TYR degradation and depigmentation in monobenzone-treated C57BL/6 mice.

4. Discussion

Thus far, only a few bioactivity or pharmacological studies on EB are available, and these studies describe the function of EB in osteoporosis treatment, nerve protection, and immune activity stimulation [20–22]. In this study, we provided comprehensive evidence of EB function in pigmentation *in vivo* and *in vitro*, using melanoma cells, human primary melanocytes, human skin-organ explant culture, and depigmented zebrafish and C57BL/6 mice; we also elucidated the multiple mechanisms regulating melanogenesis by increasing TYR expression, activity, and stability.

Melanogenesis is a complex process involving different stages and occurs in melanosomes [4]. Generally, the number of melanocytes in all types of human skin is basically constant, and the number, size, and maturation stage of melanosomes determine differences in pigmentation [23]. Our data demonstrated that EB increased melanosome number and promoted melanosome maturation to regulate melanin production. In mammalian melanocytes, mature melanosomes are transported from the perinuclear area to cell periphery, and from the periphery, they are further transferred to adjacent keratinocytes by actin- and microtubule-dependent dendrites [24]. However, we did not observe any intuitive changes in melanocyte dendrites and transport regulator proteins after EB treatment, which indicated that EB has a lesser effect on the events of melanin transfer from melanocytes to keratinocytes, although intramelanocytic melanosome transport has been realized based on our data. Hence, this study focused on melanocytic biological processes responsible for EB-induced melanin biosynthesis.

Both eumelanin and pheomelanin are synthesized through a series of reactions that are initiated by the oxidation of tyrosine to dopaquinone, catalyzed by TYR [12,25–27]. After the common obligatory step, TYRP1 and DCT further modify melanin into eumelanin. We did not perform the absolute analysis of pigment types, but the remarkably upregulated mRNA and protein expression of TYRP1 and DCT implies that eumelanin content may account for a considerable part of EB-induced mixed pigments.

Initial melanosomes are formed in the perinuclear region near the Golgi apparatus and receive various structural and enzymatic proteins required for melanogenesis. Stage I melanosomes are spherical vacuoles that have no TYR and internal structural components. Subsequently, TYR are trafficked to stage II melanosomes that have minimal melanin deposition. Melanin begins to synthesize at stage III melanosomes, and is uniformly deposited on the internal fibrils. Stage IV melanosomes are highly opaque, which feature as complete melanization and elliptical/ellipsoidal shape, and have minimal TYR activity [24]. In our results, the time inconsistency of the peak value of melanin content and TYR activity caused by EB can be well attributed to the melanosome melanization process: 1) the sharp increase in melanin content until 72 h is because melanin synthesis starts in stage III melanosomes, for which numerous events (structural shape, enzyme synthesis, transport, and trafficking) have to be completed; 2) melanin production is a progressive process (synthesis, accumulation, and deposit); however, TYR activation initiated in early-

Fig. 8. Epimedin B (EB) improves tyrosinase (TYR) and TYR-related protein 1 (TYRP1) stability by affecting the ubiquitin-proteasome degradation pathway. (A) The protein expression levels of TYR, TYRP1, and dopachrome tautomerase (DCT) (cycloheximide (CHX): 50 μg/mL; monobenzone: 30 μM; EB: 100 μM for 0, 6, 12, and 24 h), and statistics for TYR, TYRP1, and DCT expression. (B) The ubiquitin expression levels of purified TYR and TYRP1 (monobenzone: 60 μM; EB: 100 μM treated for 6 h). (C) The calnexin expression levels of purified TYR and TYRP1 (monobenzone: 60 μM; EB: 100 μM treated for 6 h). (D) Representative images of immunofluorescence staining on B16F10 cells (red: TYR: calnexin complex, blue: 4′,6-diamidino-2-phenylindole (DAPI); monobenzone: 60 μM, EB: 100 μM treated for 6 h). (E) Representative images of immunofluorescence staining on B16F10 cells (red: calnexin, green: TYR, blue: DAPI; monobenzone: 60 μM, EB: 100 μM treated for 6 h). (F) Representative images of immunofluorescence staining on B16F10 cells (red: 26S proteasome α, green: TYR, blue: DAPI; monobenzone: 60 μM and EB: 100 μM treated for 12 h). For graphical representation, data are presented as mean ± standard error of the mean ($n \geq 3$ in each group). $P < 0.05$, $P < 0.01$, and $P < 0.001$ vs. control (CTRL) are considered to be significant. Representative image from three independent experiments is shown. DMSO: dimethyl sulfoxide; IP: immunoprecipitation.
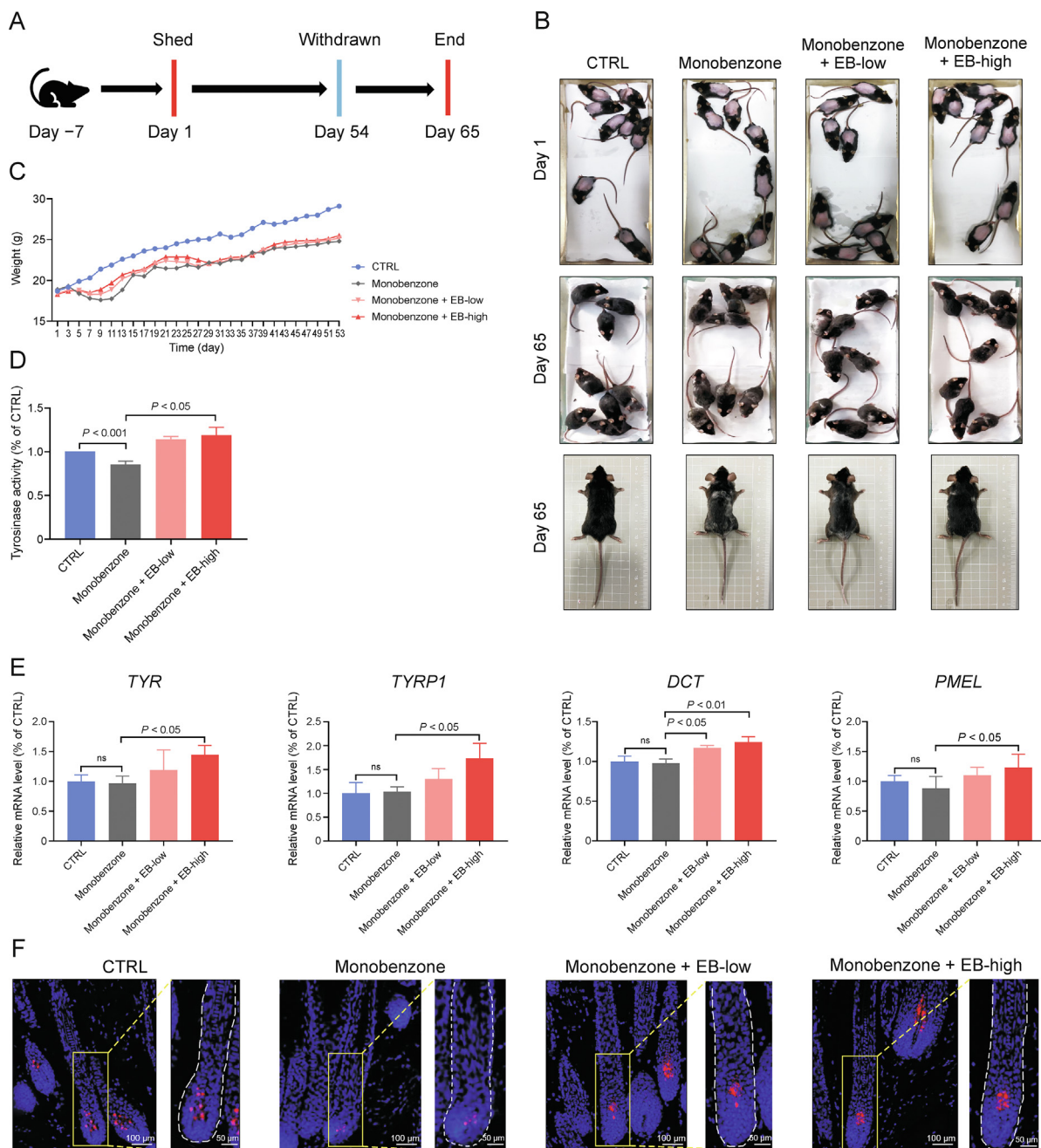
Fig. 9. Epimedin B (EB) can ameliorate monobenzone-induced depigmentation in C57BL/6 mice. (A) Timeline of mice experiment procedure. (B) Images of C57BL/6 mice dorsal hair color. (C) Statistic for mice bodyweight. (D) Tyrosinase (TYR) activity of mice dorsal skin. (E) The messenger RNA (mRNA) expression levels of *TYR*, TYR-related protein 1 (*TYRP1*), dopachrome tautomerase (*DCT*), and premelanosome protein (*PMEL*). (F) Representative images of immunofluorescence staining of hair follicles with TYR. For graphical representation, data are presented as mean ± standard error of the mean ($n \geq 3$ in each group). $P < 0.05$, $P < 0.01$, and $P < 0.001$ vs. control (CTRL) are considered to be significant. Representative image from three independent experiments is shown.

stage melanosomes; thus, TYR activity peaked earlier than melanin content maximum; and 3) the decreasing trend of TYR activity at 72 h is attributed to the fact that, at this time point, melanosome melanization has finished.

Although the endogenous degradation of TYR controls melanogenesis, little mechanism of TYR degradation induced by exogenous chemicals had been clarified. ERAD-mediated ubiquitin-proteasome proteolysis was reported to be involved in TYR degradation event [17,28]. Newly synthesized TYR has a molecular mass of 55–58 kDa, and TYRP1 and DCT have a molecular mass of

approximately 55 kDa. After post-translational folding and trafficking to the Golgi apparatus for further processing, the mature and glycosylated TYR increases in mass to 65–75 kDa and glycosylated TYRP1 and DCT increase to a mass of 70–75 kDa and even more higher [23]. Our data showed that, compared with natural TYRs, monobenzone treatment exactly aggravates the generation of aberrant TYRs (TYR and TYRP1 with a mass of approximately 60 kDa; DCT with a mass of approximately 55 and 43 kDa) by altering their glycosylation. Simultaneously, EB ameliorates the formation of aberrant TYR and TYRP1 proteins. Therefore, to some

extent, these data imply that EB has the influence of inhibiting monobenzone-induced deglycosylation on TYR/TYRP1, causing retention of aberrant TYR/TYRP1 in the ER and leading to ubiquitination. It is also worth noting that, in addition to its catalytic function in oxidizing dihydroxyindolecarboxylic acid, TYRP1 may play an important role in regulating TYR activity and stabilizing TYR, which serves as a second potential role in the regulation of melanin synthesis [12]. Thus, we infer that EB-induced TYR improvements are related to the protective function of TYRP1.

However, there are still certain issues that remain to be further explored. 1) Previous studies demonstrated that TYR activity can be regulated by interactions with cysteine, involving chelation of two copper ions, by competitive occupancy of the catalytic site [23,29]. Yet, the mechanism underlying EB-induced TYR activity remains unexplored. 2) Although ERAD-mediated protein degradation has been reported for DCT, the mechanism of EB-induced protective effect on DCT degradation is probably different. It remains unclear whether it is related to other degradation approaches induced by monobenzone from the autophagy pathway and whether the endosomal/lysosomal system, which have been studied before, is involved [16]. 3) The association between multiple effects of TYRs induced by EB is unclear. Previous studies reported that nicotinamide nucleotide transhydrogenase, a mitochondrial redox-regulating enzyme, plays a key role in modulating TYR expression, activity, and stability [30]. We speculate whether nicotinamide nucleotide transhydrogenase or other similar proteins with unknown function are regulated by EB and then influence the downstream TYRs.

5. Conclusion

In conclusion, we demonstrated that EB exerted pigmentation function *in vivo* and *in vitro*. The pigmentation mechanism of EB occurs through three pathways: 1) EB increased TYR expression by p-AKT-mediated GSK3β/β-catenin pathway, p-p70 S6 kinase cascade, and p38/MAPK and ERK/MAPK pathways and enhanced melanosome number and maturation stage; 2) EB activated TYR activity; and 3) EB enhanced TYRs stability by preventing the formation of aberrant TYR and TYRP1 and their retention in the ER, and inhibiting ubiquitin-proteasome degradation. These data indicate that EB can target TYRs in terms of expression, catalytic activity, and stability to exhibit pigmentation function, which might provide a novel rational strategy for hypopigmentation in the pharmaceutical and cosmetic industries.

CRediT author statement

Chen Hong: Investigation, Methodology, Writing - Original draft preparation; **Yifan Zhang:** Formal analysis, Data curation; **Lili Yang:** Resources, Investigation; **Haoyang Xu:** Methodology, Software; **Kang Cheng** and **Zhi Lv:** Conceptualization, Resources; **Kaixian Chen:** Resources, Project administration; **Yiming Li:** Funding acquisition, Project administration, Supervision; **Huali Wu:** Conceptualization, Methodology, Investigation, Supervision, Writing - Reviewing and Editing.

Declaration of competing interest

The authors declare that there are no conflicts of interest.

Acknowledgments

Appendix A. Supplementary data

Supplementary data to this article can be found online at https://doi.org/10.1016/j.jpha.2023.09.006.

References

[1] S.A. D'Mello, G.J. Finlay, B.C. Baguley, et al., Signaling pathways in melanogenesis, Int. J. Mol. Sci. 17 (2016), 1144.

[2] X. Tian, Z. Cui, S. Liu, et al., Melanosome transport and regulation in development and disease, Pharmacol. Ther. 219 (2021), 107707.

[3] S. Benito-Martínez, L. Salavessa, G. Raposo, et al., Melanin transfer and fate within keratinocytes in human skin pigmentation, Integr. Comp. Biol. 61 (2021) 1546—1555.

[4] I.F. Videira, D.F. Moura, S. Magina, Mechanisms regulating melanogenesis, An. Bras. Dermatol. 88 (2013) 76—83.

[5] N. Arora, E.M. Siddiqui, S. Mehan, Involvement of adenylate cyclase/cAMP/CREB and SOX9/MITF in melanogenesis to prevent vitiligo, Mol. Cell. Biochem. 476 (2021) 1401—1409.

[6] H. Ando, H. Kondoh, M. Ichihashi, et al., Approaches to identify inhibitors of melanin biosynthesis via the quality control of tyrosinase, J. Invest. Dermatol. 127 (2007) 751—761.

[7] R. Halaban, E. Cheng, Y. Zhang, et al., Aberrant retention of tyrosinase in the endoplasmic reticulum mediates accelerated degradation of the enzyme and contributes to the dedifferentiated phenotype of amelanotic melanoma cells, Proc. Natl. Acad. Sci. U S A 94 (1997) 6210—6215.

[8] C. Hong, L. Yang, Y. Zhang, et al., *Epimedium brevicornum* Maxim. extract exhibits pigmentation by melanin biosynthesis and melanosome biogenesis/transfer, Front. Pharmacol. 13 (2022), 963160.

[9] H. Tang, L. Yang, L. Wu, et al., Kaempferol, the melanogenic component of *Sanguisorba officinalis*, enhances dendricity and melanosome maturation/transport in melanocytes, J. Pharmacol. Sci. 147 (2021) 348—357.

[10] D. Hu, Methodology for evaluation of melanin content and production of pigment cells in vitro, Photochem. Photobiol. 84 (2008) 645—649.

[11] Y.S. Su, Z.X. Fan, S.E. Xiao, et al., Icariin promotes mouse hair follicle growth by increasing insulin-like growth factor 1 expression in dermal papillary cells, Clin. Exp. Dermatol. 42 (2017) 287—294.

[12] L. Le, J. Sirés-Campos, G. Raposo, et al., Melanosome biogenesis in the pigmentation of mammalian skin, Integr. Comp. Biol. 61 (2021) 1517—1545.

[13] D. Kim, H.J. Kim, H.S. Jun, *Polygonum multiflorum* thunb. extract stimulates melanogenesis by induction of COX2 expression through the activation of p38 MAPK in B16F10 mouse melanoma cells, Evid. Based Complement. Alternat. Med. 2020 (2020), 7642019.

[14] C. Niu, H.A. Aisa, Upregulation of melanogenesis and tyrosinase activity: Potential agents for vitiligo, Molecules 22 (2017), 1303.

[15] J.E. Harris, Chemical-induced vitiligo, Dermatol. Clin. 35 (2017) 151—161.

[16] J.G. van den Boorn, D.I. Picavet, P.F. van Swieten, et al., Skin-depigmenting agent monobenzone induces potent T-cell autoimmunity toward pigmented cells by tyrosinase haptenation and melanosome autophagy, J. Invest. Dermatol. 131 (2011) 1240—1251.

[17] S. Svedine, T. Wang, R. Halaban, et al., Carbohydrates act as sorting determinants in ER-associated degradation of tyrosinase, J. Cell Sci. 117 (2004) 2937—2949.

[18] Y. Zhu, S. Wang, A. Xu, A mouse model of vitiligo induced by monobenzone, Exp. Dermatol. 22 (2013) 499—501.

[19] R. Speeckaert, S. Voet, E. Hoste, et al., S100B is a potential disease activity marker in nonsegmental vitiligo, J. Invest. Dermatol. 137 (2017) 1445—1453.

[20] X. Diao, L. Wang, Y. Zhou, et al., The mechanism of Epimedin B in treating osteoporosis as revealed by RNA sequencing-based analysis, Basic Clin. Pharmacol. Toxicol. 129 (2021) 450—461.

[21] M. Zhang, Z. Hu, X. Dong, et al., Epimedin B exerts neuroprotective effect against MPTP-induced mouse model of Parkinson's disease: GPER as a potential target, Biomed. Pharmacother. 156 (2022), 113955.

[22] Y. Gao, W. Shi, C. Tu, et al., Immunostimulatory activity and structure-activity relationship of epimedin B from *Epimedium brevicornu* Maxim, Front. Pharmacol. 13 (2022), 1015846.

[23] A. Slominski, D.J. Tobin, S. Shibahara, et al., Melanin pigmentation in mammalian skin and its hormonal regulation, Physiol. Rev. 84 (2004) 1155—1228.

[24] G.E. Costin, V.J. Hearing, Human skin pigmentation: Melanocytes modulate skin color in response to stress, FASEB. J. 21 (2007) 976—994.

[25] C.J. Cooksey, P.J. Garratt, E.J. Land, et al., Evidence of the indirect formation of the catecholic intermediate substrate responsible for the autoactivation kinetics of tyrosinase, J. Biol. Chem. 272 (1997) 26226—26235.

[26] C.A. Ramsden, P.A. Riley, Tyrosinase: The four oxidation states of the active site and their relevance to enzymatic activation, oxidation and inactivation, Bioorg. Med. Chem. 22 (2014) 2388—2395.

[27] H.S. Mason, The chemistry of melanin; mechanism of the oxidation of dihydroxyphenylalanine by tyrosinase, J. Biol. Chem. 172 (1948) 83—99.

[28] Y. Wang, M.J. Androlewicz, Oligosaccharide trimming plays a role in the endoplasmic reticulum-associated degradation of tyrosinase, Biochem. Biophys. Res. Commun. 271 (2000) 22—27.

[29] M. Furumura, F. Solano, N. Matsunaga, et al., Metal ligand-binding specificities of the tyrosinase-related proteins, Biochem. Biophys. Res. Commun. 242 (1998) 579—585.

[30] J. Allouche, I. Rachmin, K. Adhikari, et al., NNT mediates redox-dependent pigmentation via a UVB- and MITF-independent mechanism, Cell 184 (2021) 4268—4283.e20.